AWARD NO.	AWARD/MODIFICATION	MODIFICATION NO.	
N00014-13-1-0258		A00001	

27. SPECIAL INSTRUCTIONS:

See "Special Requirements" Attachment

28. DELEGATIONS: The administration duties listed below have been delegated to the administrative office (block 23a). Upon request the awarding office contact (block 22) will make their full text available. Please direct questions to the contacts @: http://www.onr.navy.mil/Contracts-Grants/Regional-Contacts.aspx

Full Delegation

29. TERMS AND CONDITIONS: The following terms and conditions are incorporated herein by reference with the same force and effect as if they were given in full text. Upon request the awarding office contact named in block 22 will make their full text available, or they can be found as described below.

DOCUMENT

The following documents may be found at:
http://www.onr.navy.mil/Contracts-Grants/submit-proposal/grants-proposal/grants-terms-conditions.aspx

Special Terms and Conditions - Policy for In Situ Ocean Data Article (October 1999)
Standard Terms and Conditions for Research Grants - June 2011 (Core)
Standard Terms and Conditions for Research Grants - February 2011 (Agency Specific)
UAAC UACC Acceptance C November
UAWA UAWA Award A

30. OPTIONS OPTION NO. AMOUNT PERIOD

(1)
(2)
(3)
(4)

31. REPORTS: The following reports must be submitted to the indicated addressees, in the indicated quantities, within 90 days following the expiration or termination of the project. Final Technical Reports must have a SF298, Report Documentation Page, accompanying them. Unless otherwise stated in the award/modification, complete Block 12a of the SF298 as follows: "Approved for Public Release; distribution is Unlimited".

ADDRESSEE	REPORT TYPE	COPIES
See block #21	Final Technical Report with SF298 Interim Research Performance Report (As Required) with SF298	1 1
See block #23a	Report of Inventions and Subcontracts - DD 882 Final Technical Report Interim Research Performance Report (As Required) Final Federal Financial Status Report - SF425 - Including Line Item 11	1 1 1 1
Defense Technical Information Center 8725 John J Kingman Road Ste 0944 Fort Belvoir, VA 22060-6218	Final Technical Report with SF298 Interim Research Performance Report (As Required) with SF298	1 1
See block #26a	Report of Inventions and Subcontracts - DD 882	1
Naval Research Laboratory ATTN: CODE 5596 4555 Overlook Avenue SW Washington, DC 20375-5320	Final Technical Report Interim Research Performance Report (As Required) with SF298	1 1

32. FOR THE RECIPIENT		33. FOR THE UNITED STATES OF AMERICA	
32a. SIGNATURE OF PERSON AUTHORIZED TO SIGN N/A - SIGNATURE NOT REQUIRED ON THIS AWARD		33a. SIGNATURE OF AWARDING OFFICER Yolanda Willett	
32b. NAME AND TITLE OF SIGNER	32c. DATE SIGNED	33b. NAME AND TITLE OF AWARD OFFICER Yolanda E. Willett	33c. DATE SIGNED 11-JUL-14

REPORT DOCUMENTATION PAGE

Form Approved
OMB No. 0704-0188

1. REPORT DATE *(DD-MM-YYYY)*	2. REPORT TYPE	3. DATES COVERED *(From - To)*
11/21/2016	Final Report	01 Jan 2013 - 30 June 2016

4. TITLE AND SUBTITLE
Multi-Resonance Shear Mode Transducers

5a. CONTRACT NUMBER

5b. GRANT NUMBER
N00014-13-1-0258

5c. PROGRAM ELEMENT NUMBER

6. AUTHOR(S)
Richard J. Meyer, Jr.

5d. PROJECT NUMBER
20733

5e. TASK NUMBER

5f. WORK UNIT NUMBER
09730

7. PERFORMING ORGANIZATION NAME(S) AND ADDRESS(ES)
Applied Research Laboratory
The Pennsylvania State University
P.O. Box 30
State College, PA 16804

8. PERFORMING ORGANIZATION REPORT NUMBER

9. SPONSORING/MONITORING AGENCY NAME(S) AND ADDRESS(ES)
Jan Lindberg and Mike Wardlaw
Office of Naval Research
Code 321MS
875 N. Randolph Street
Arlington, VA 22203

10. SPONSOR/MONITOR'S ACRONYM(S)
ONR

11. SPONSOR/MONITOR'S REPORT NUMBER(S)

12. DISTRIBUTION/AVAILABILITY STATEMENT

13. SUPPLEMENTARY NOTES

14. ABSTRACT

Crystallographic engineering of single crystal relaxor-based ferroelectrics was used to design broadband, compact, high power, low frequency transducers. A unique face shear-mode produces a d36 coefficient that has demonstrated the ability provide a robust projector that meets these qualifications. This work looks at expanding the operating bandwidth and/or acoustic power output that may be achieved by designing multi-mode transducers using multiple d36 crystal geometries or combinations of d36 and other crystal cuts.

15. SUBJECT TERMS

16. SECURITY CLASSIFICATION OF:			17. LIMITATION OF ABSTRACT	18. NUMBER OF PAGES	19a. NAME OF RESPONSIBLE PERSON
a. REPORT	b. ABSTRACT	c. THIS PAGE			Richard J. Meyer, Jr.
Unclassified	Unclassified	Unclassified	UNCLASSIFIED	24	19b. TELEPHONE NUMBER *(Include area code)* 814-865-9607

DISTRIBUTION STATEMENT A

Multi-Resonance Shear Mode Transducers

Grant: N00014-13-1-0258
Start Date: 01 Jan 2013
End Date: 30 Jun 2016
Principal Investigator: Richard J. Meyer Jr.

Final Report

21 November 2016

PENNSTATE

Applied Research Laboratory

Submitted to:

Jan Lindberg and Mike Wardlaw
ONR Code 321MS
875 N Randolph Street
Arlington, VA 22203

Submitted by:

The Pennsylvania State University
Applied Research Laboratory
P.O. Box 30
State College, PA 16804-0030
R. J. Meyer Jr.
(814) 865-9607
rjm150@arl.psu.edu

Multi-Resonance Shear Mode Transducers

Prepared by: Douglas Markley

LONG-TERM GOALS

The long-term goals of this effort were to develop a family of transducer designs that utilize the d_{36} shear piezoelectric coefficient, which has advantages for compact low frequency sonar transducers. The d_{36} cut is unique in that large electric fields can be applied without depolarization. The d_{36} mode of operation allows for packaging of a transducer motor section that is unlike any other and therefore a new design space is offered to the designer. This effort looks specifically at designing a d_{36} transducer that has multiple resonances in order to expand the useful transmit frequency bandwidth.

OBJECTIVES

The primary technical objective was to exploit crystallographic engineering of single crystal relaxor-based ferroelectrics to design broadband, compact, high power, low frequency transducers. Face shear-mode transducers based on the d_{36} coefficient have demonstrated the ability to design a robust projector that meets these qualifications. Further expanding the operating bandwidth and/or acoustic power output may be achieved by designing multi-mode transducers using multiple d_{36} crystal geometries or combinations of d_{36} and other crystal cuts.

APPROACH

Traditional approaches to compact sonar projector design usually involve mechanical amplification schemes or bending modes of the active material. Structures using mechanical amplification tend to be very narrow band and have low electromechanical coupling coefficients. Bending modes are also traditionally narrow band and generally have long-term reliability issues. While implementing single crystal materials into these structures improves performance, the full electromechanical coupling of the material is still degraded.

Crystallographic engineering in the single crystal lead magnesium niobate-lead titanate (PMNT) system has uncovered a very unique piezoelectric shear mode. Contrary to other more common shear coefficients, this one operates with working electrodes that are the same as the poling electrodes. Therefore, very large driving fields can be applied to the device without depolarization. This mode of operation is not available in conventional piezoceramics. This cut was recently integrated into a sonar transducer design that combines low frequency operation with small packaging and high acoustic output.

There is a significant design space left to explore with this new mode of operation. This study focused on the ability to design multiple resonances into the structure to tailor the performance of the device. Multiple resonances can be combined to improve output or lower the frequency of

operation or can be separated to extend the operating bandwidth of the device. Modeling, both one dimensional and finite element analysis, was used to explore the design space. Prototype designs were fabricated and tested for proof of concept.

The design shown in Figure 1 has d36 mode crystals separated into two motor sections. The components of this design concept include a light/stiff head mass (dark gray), a heavy tail mass (light gray), d_{36} crystals (black), and a central mass (cross-hatched). The resonance frequency of each motor section can be controlled through the dimensions (width, height or length) of the crystal plates. In this case, the two motor sections can be combined to lower the resonance frequency (mechanical springs in series) or they can be designed at different frequencies to create a multi-resonant spectrum and thereby increasing the bandwidth of the projector.

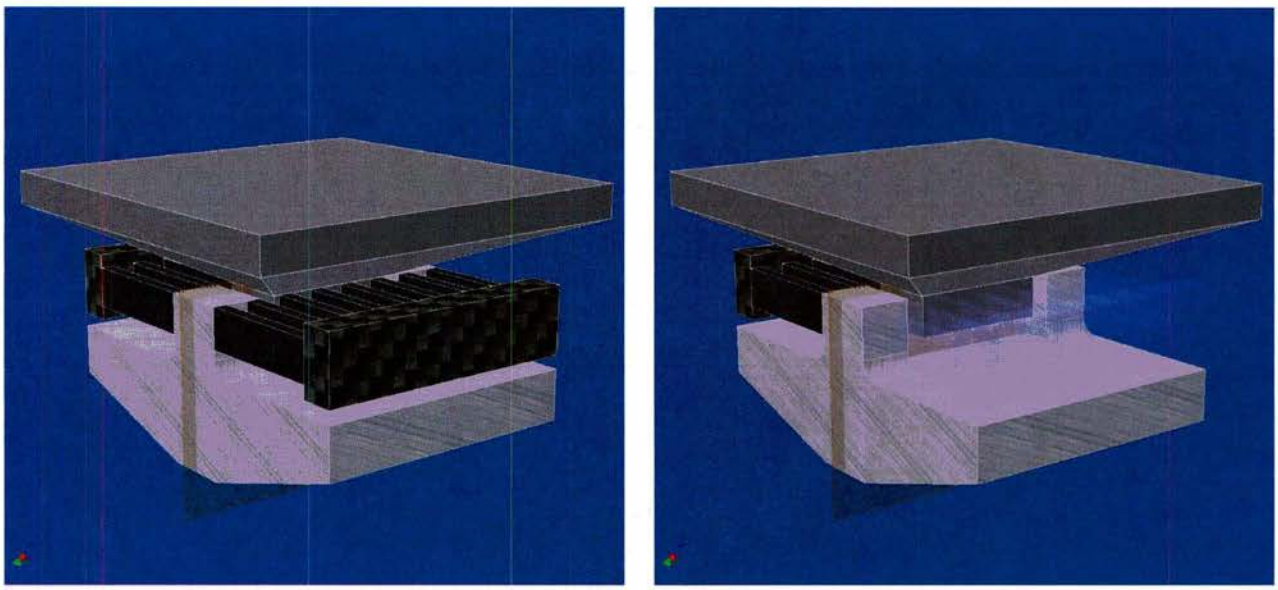

Figure 1 Multi-mode transducer; both sections use longitudinal shear crystals. (Left) full transducer with dark gray head, light gray tail, crystals in solid black, and center support in back cross-hatch. (Right) is a cut-view showing nested head and tail.

WORK COMPLETED

An equivalent circuit model of d_{36} shear mode transducers was developed to more rapidly explore transducer design space. The model considers a mass-spring-mass-spring-mass system. The model was exercised and compared to results obtained using finite element analysis.

Based on equivalent circuit analysis, final geometries were then modeled using ATILA++ finite element code. Refinements were made to the central mass geometry and materials to produce a desirable frequency response curve.

As an example of this process, a dual-shear mode transducer was constructed that measured 1.5 inches in diameter and was 2.75 inches in length. In air impedance sweeps were measured

during each stage of fabrication and compared to model results to ensure fabrication proceeded as expected. A cut-away model and photograph of the finished unit is shown in Figure 2

Part drawings were produced and parts were procured. d_{36} crystals were obtained from HC Materials. Crystals were inspected, measured, and sorted for use in the transducer design and evaluated for proper motion using a scanning laser vibrometer.

In-air testing was done on the finished unit. These data were compared to model predictions.

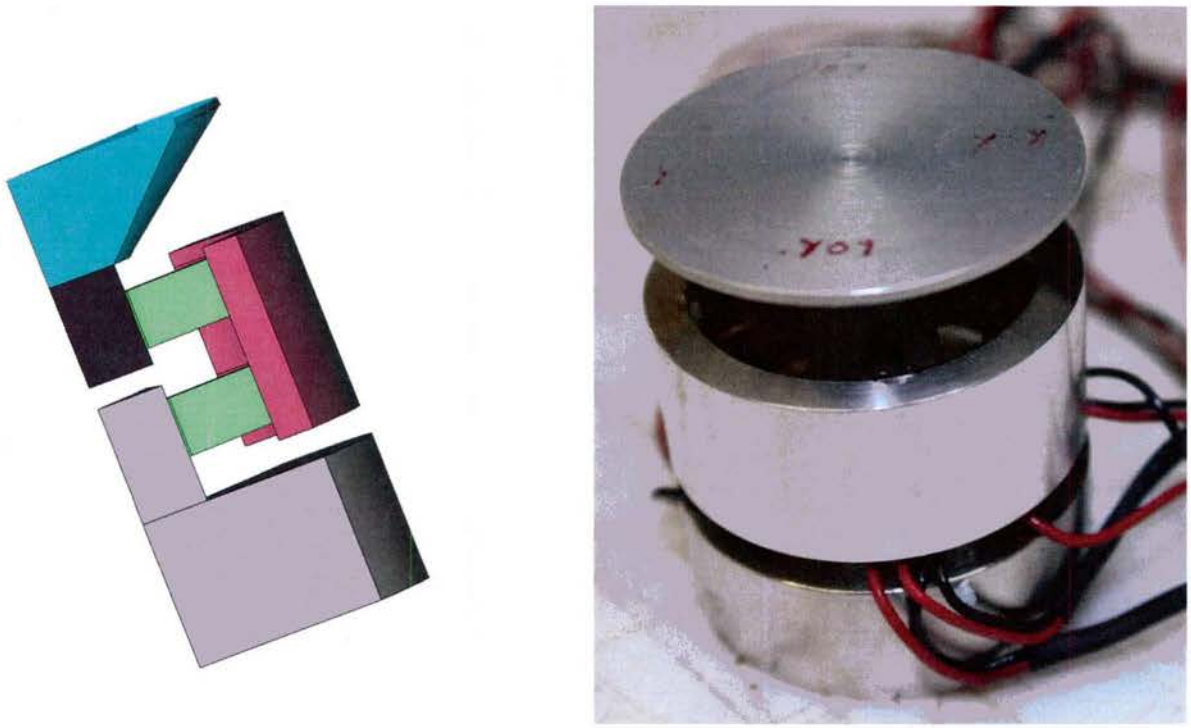

Figure 2 Model (1/4 symmetry) and photograph of the assembled dual stage d_{36} tonpilz transducer.

In-water testing of the unit was conducted by placing the unit in a single element housing. The unit was tested in water by driving the bottom and top d36 stages in phase and then the lower d36 stages was driven 180° out of phase.

Many other design configurations were explored in modeling studies to take advantage of the unique properties of d_{36} orientated single crystals. One such design uses an alternate positioning of the crystals and allows for utilizing the d_{36} mode in an axial direction (free-shear) to build devices similar to classical tonpilz designs. This new approach permits simpler fabrication and allows for the use of pre-stress bolts. Single and Dual-Mode prototypes of this concept were constructed and evaluated.

RESULTS

Figure 3 shows an example of the modeled response curve for the multi-mode d_{36} prototype in Figure 2. Two d_{36} shear crystal drivers are configured in series with a center-mass between. The

output is shown when the top and bottom sections are driven in phase. The modeled deflection shapes are also shown. The null in mid-band results when the central mass moves out-of-phase with the head and tail. The motion can be adjusted through design and material choices for the central mass and crystals. The null can also be countered by phasing the drive signals between the top and bottom crystal stages, preventing the phase synchronization. This is shown in Figure 4, where the drive voltage phase of the bottom stage was adjusted relative to the top stage in the models.

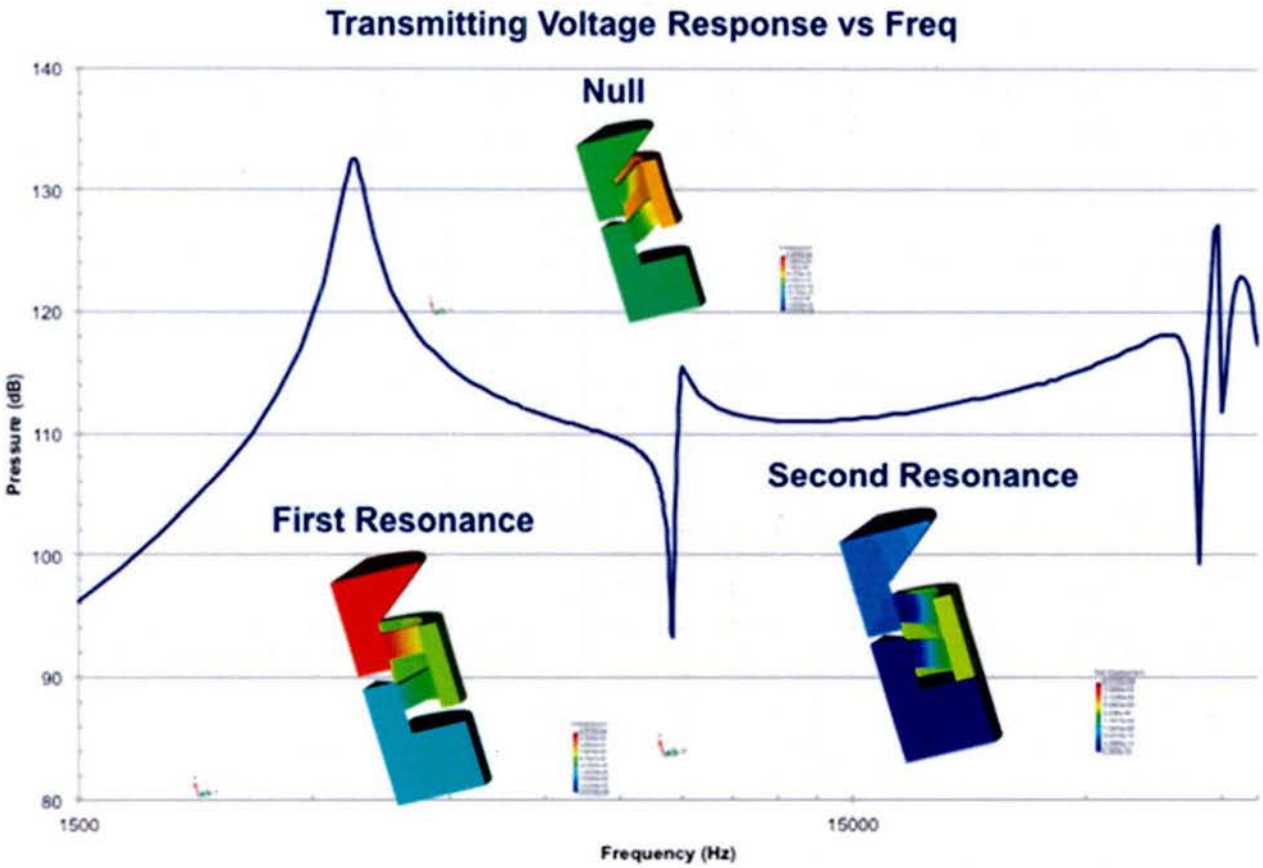

Figure 3 Modeled transmit voltage response showing the fundamental resonance of the device and overtones.

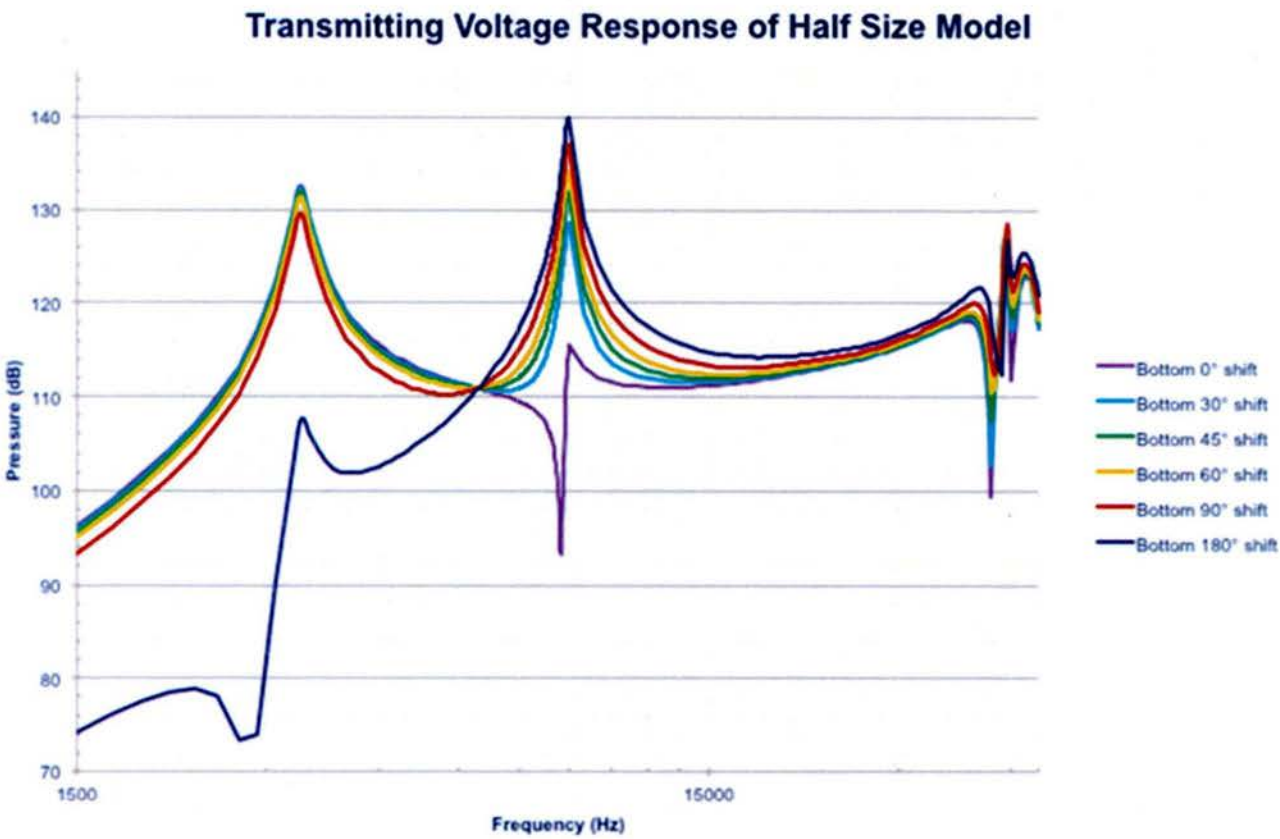

Figure 4 TVR showing the effect of adjusting the drive-phase of the bottom stage relative to the top.

Figure 5 shows the transducer during fabrication. The top and bottom stages were assembled separately and then combined during the final fabrication step. The top and bottom stages were built using the same single crystal geometry. The crystals in the top and bottom stages were sorted to have the most uniform properties within the stages. At each stage of fabrication, the impedance was checked and compared against prediction. Figure 6 shows the impedance of the finished unit in air measured in free conditions and in the housing used for in water testing.

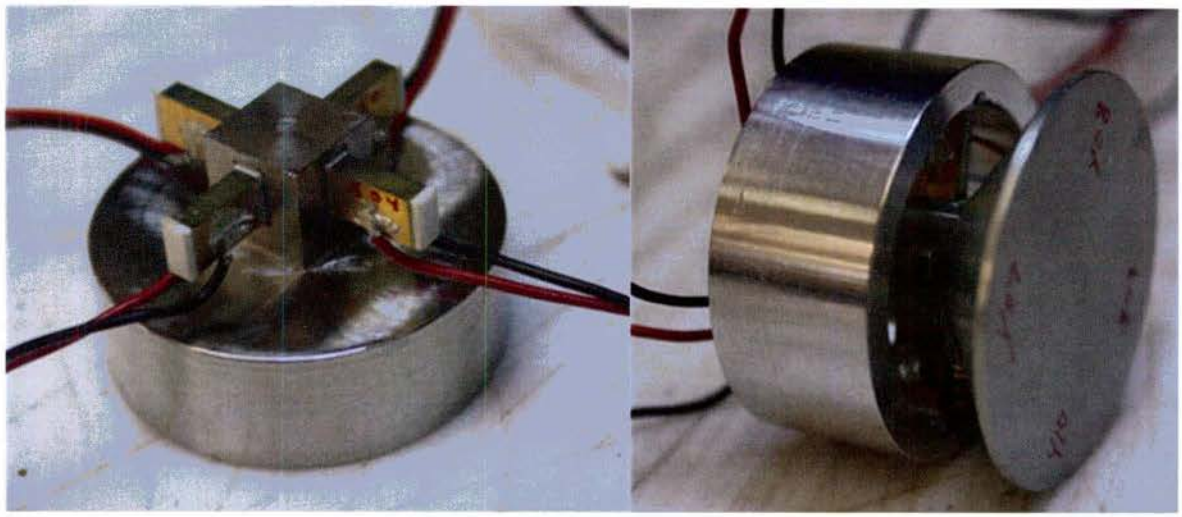

Figure 5 Photos of the bottom and top stages during the fabrication process.

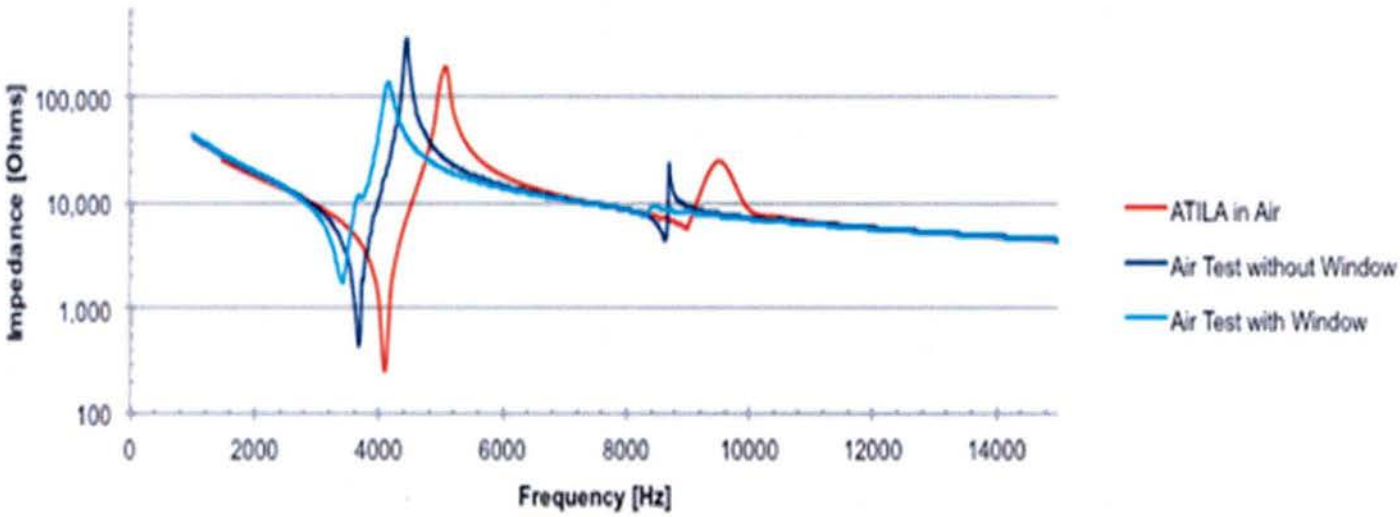

Figure 6 Measured vs. modeled in-air impedance of dual-shear prototype.

In water testing results are shown in Figure 7 and Figure 8. A reasonable match was achieved, in spite of some low frequency noise that was believed to be attributable to spurious modes in the housing structure.

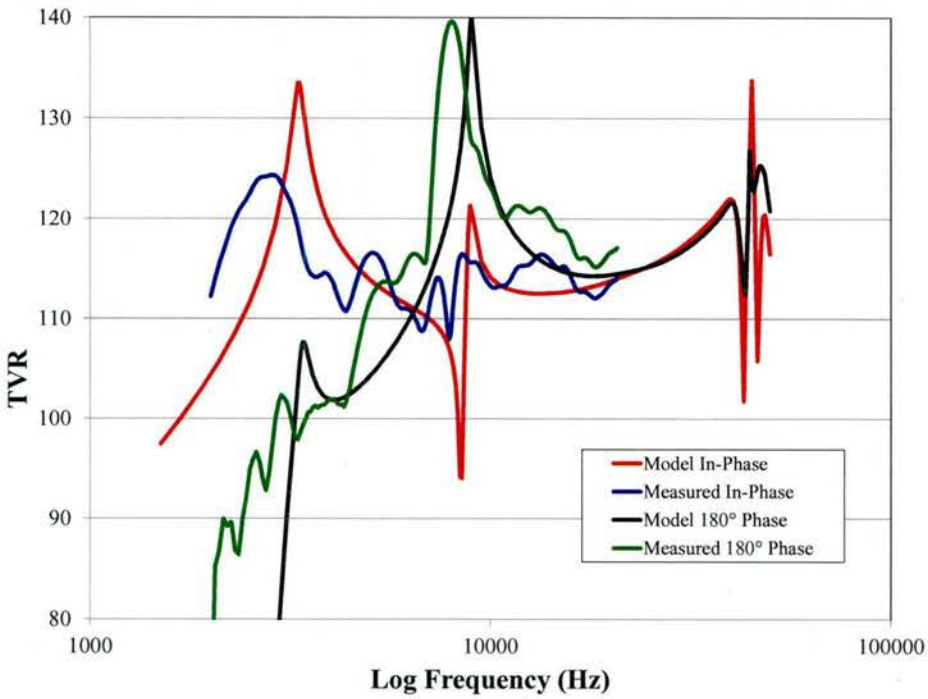

Figure 7 Measured and modeled TVR of dual-shear prototype.

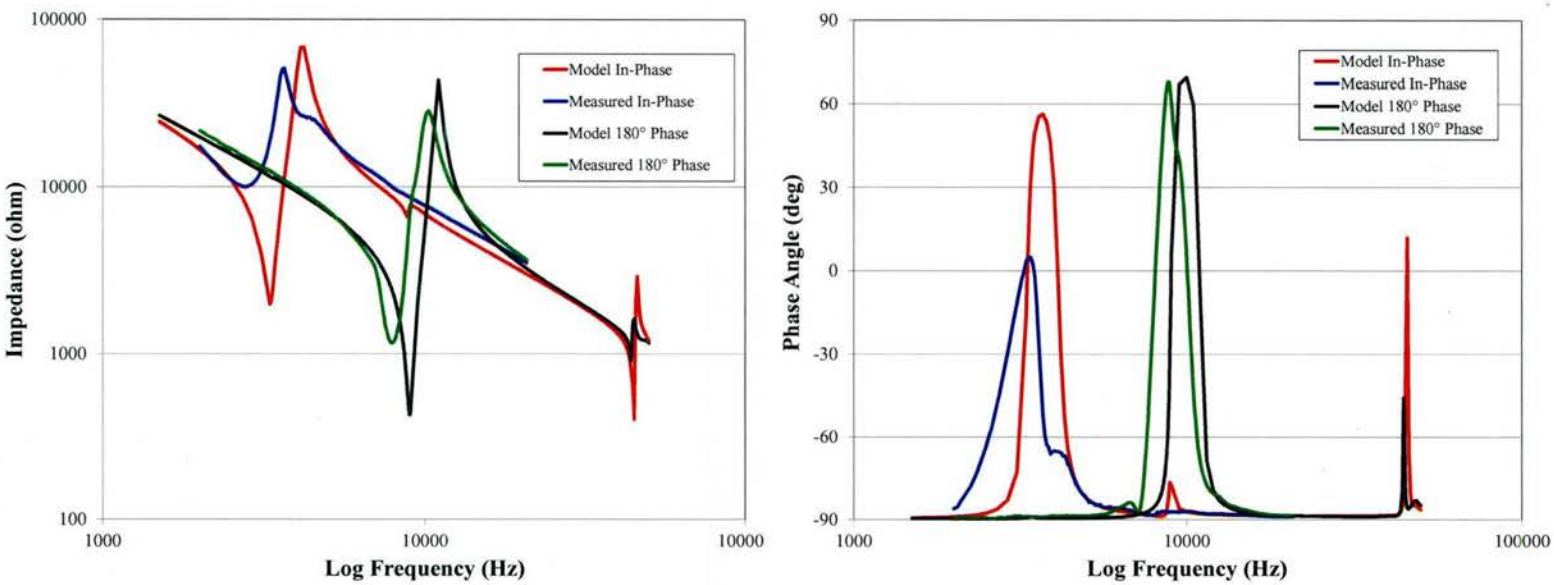

Figure 8 Measured and modeled in-water impedance and phase of the dual-shear prototype.

The design above has the two crystal drivers in a series configuration. Some other conceptual design variations that were modeled are shown below. These designs provide options that might be adjusted to meet the needs of a variety of applications in terms of acoustic performance, and physical/dimensional design constraints.

In another true series configuration (Figure 9) a stack of d_{33} crystals is located between the shear crystals and the tailmass. This is a quarter symmetry model, so it would actually require four stacks, etc. In this case the center-mass flexes in a rocking motion that is not overcome by phasing the drivers.

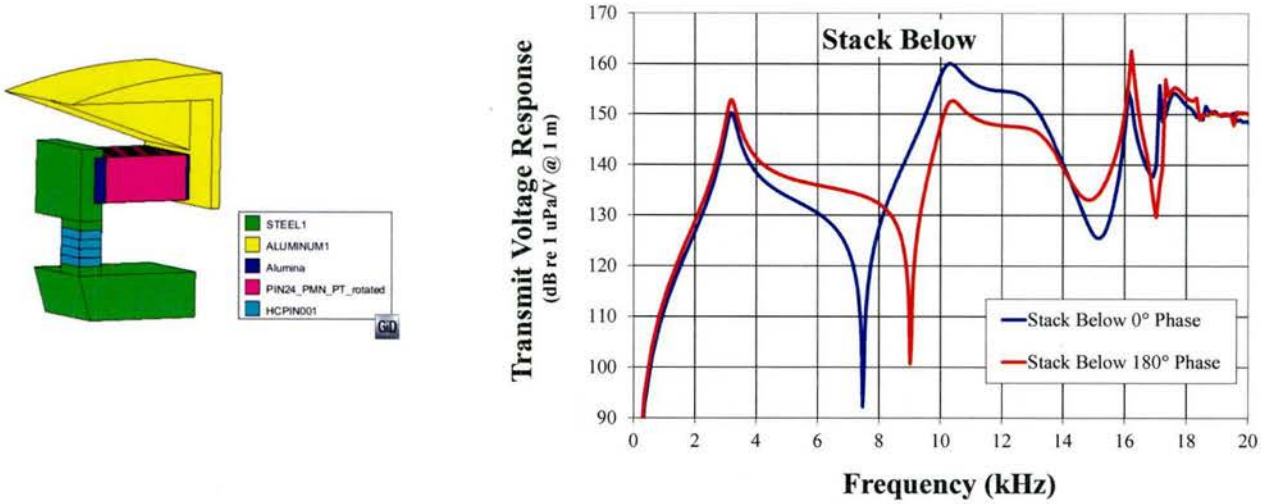

Figure 9 Dual mode transducer with d33 stacks below the shear section. (1/4 symmetry shown.)

Figure 10 shows two layers of shear crystals in series, with cantilever motion, to drive a square head. Like the prototype above, this results in an extra low fundamental resonance frequency, doubling the effective length of the crystal section. In the base configuration the preferred motion of the crystals is in opposition, spreading the head and tail masses apart. The out-of-phase coupler mode (≈3500 Hz) fights against the preferred motion and is therefore weak in this case due to the stiffness of the crystals. Note the change in behavior when the drive polarity is altered. By reversing the polarity of one set of crystals the two layers of crystal prefer to move in parallel, and a synergistic mode is formed that releases a fuller motion of the coupler. The counter balancing of the main body against the motion of the coupler causes vibration in the head for a second mode. If the drive phase is switched at the appropriate frequency during a sweep, the resulting TVR will show two peaks.

Figure 11 shows a similar concept, only this time the center mass is "Folded" back under one of the stacks for smaller cross-sectional dimensions. It too shows very low resonance frequency and strong effects from polarity reversals, showing two peaks with polarity reversal.

Figure 12 illustrates a means of achieving broad-band response by driving the devices with different polarities through different frequency ranges.

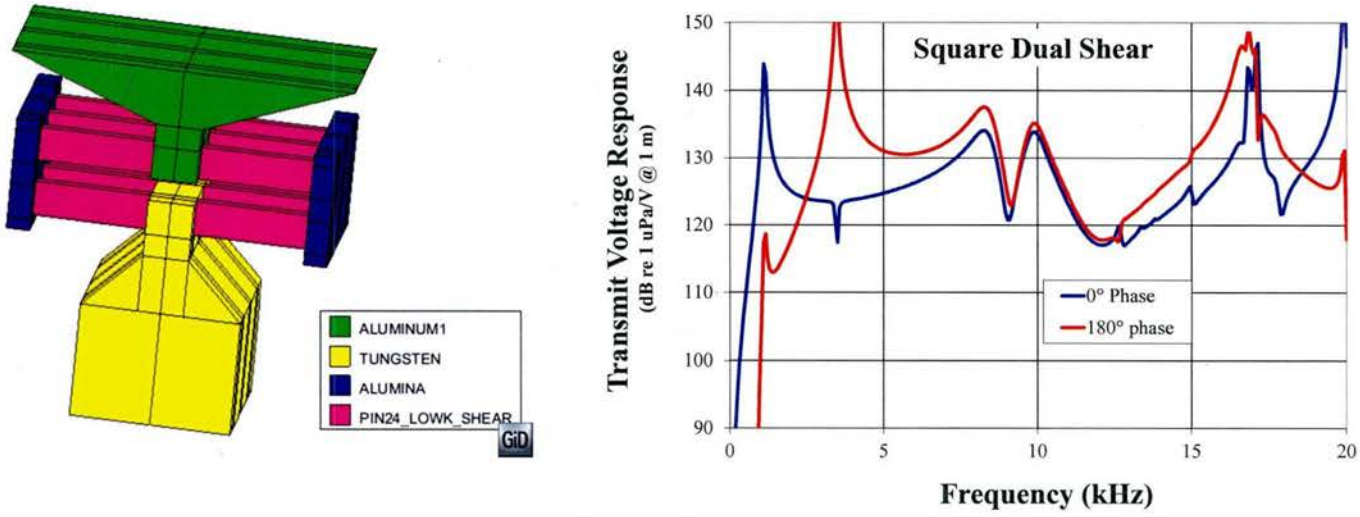

Figure 10 Two series layers of shear crystals. (1/2 symmetry shown.)

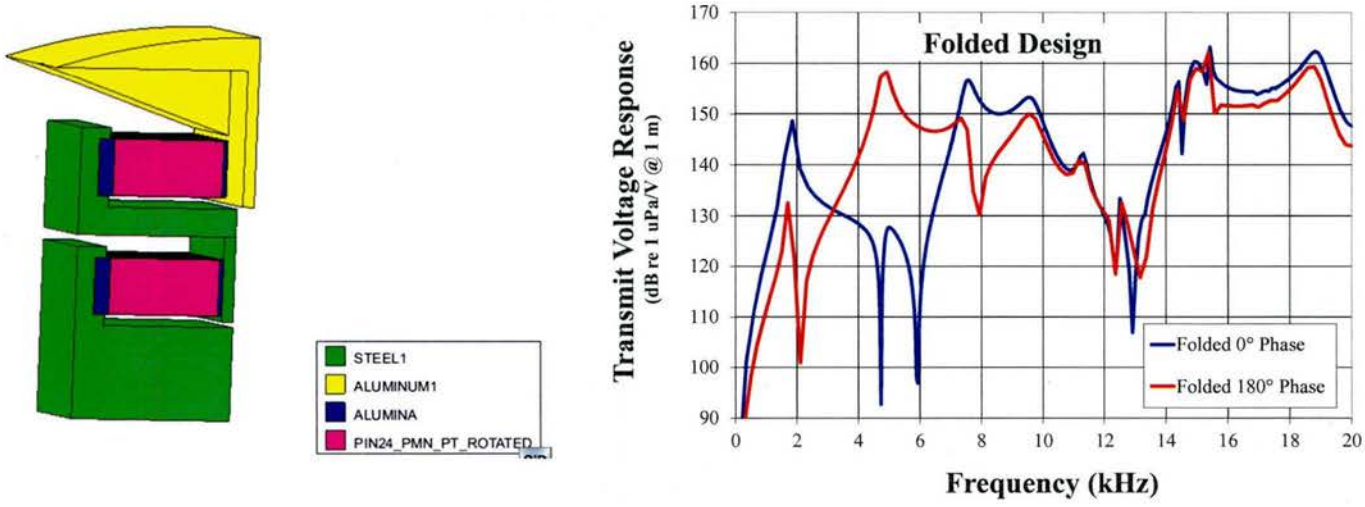

Figure 11 Dual layer shear design with one layer folded under the other. (1/4 symmetry shown.)

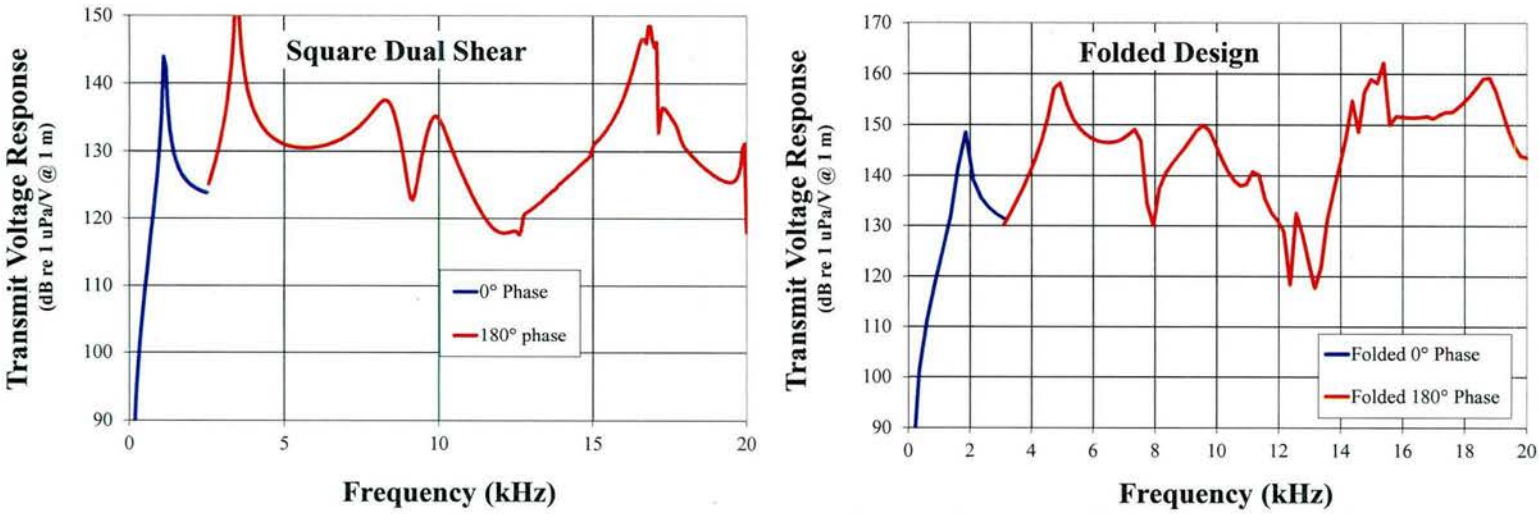

Figure 12 Increased bandwidth resulting from drive polarity adjustment.

Adjusting the dimensions of the crystal sections allows for tailoring of the results. In Figure 13 a version of the "Square Dual" design is shown where the top row of crystals is 1" X 0.3" X 0.1", and the bottom row crystals are 1" X 0.5" X 0.1". Here the upper layer is now somewhat softer and the resulting increased coupler motion can drive the head for a second mode. The 180° voltage phasing drives the coupler mode even more strongly and has some benefit at frequencies above the two main resonances.

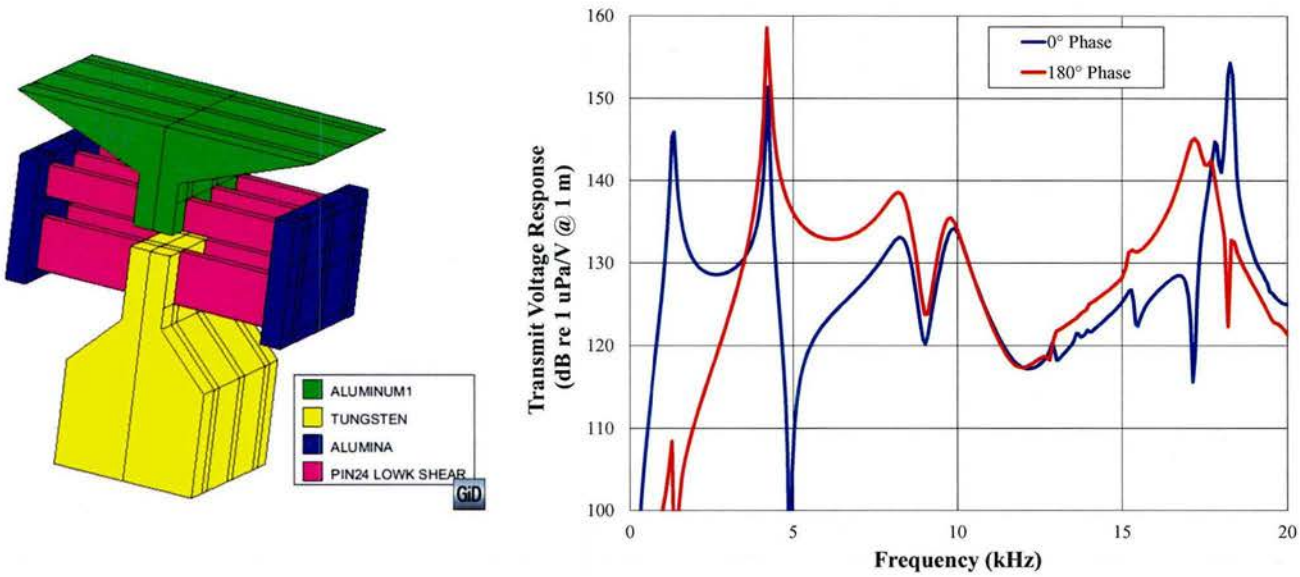

Figure 13 Square Dual-Shear with reduced width in the upper set of crystals (1/2 symmetry).

Another dual-layer cantilever configuration, this time with the bridging mass in the interior, is shown in Figure 14 together with the TVR results with all in phase or with one layer 180° out of phase with the other. In this case the bridging/coupler mass is an alumina sleeve through which a bolt may pass if desired. As before, reversing the polarity of one section enhances the coupler motion to create a second mode. Again, reducing the width of the upper set of crystals releases the coupler mode sufficiently to allow it to drive the second mode (Figure 15)

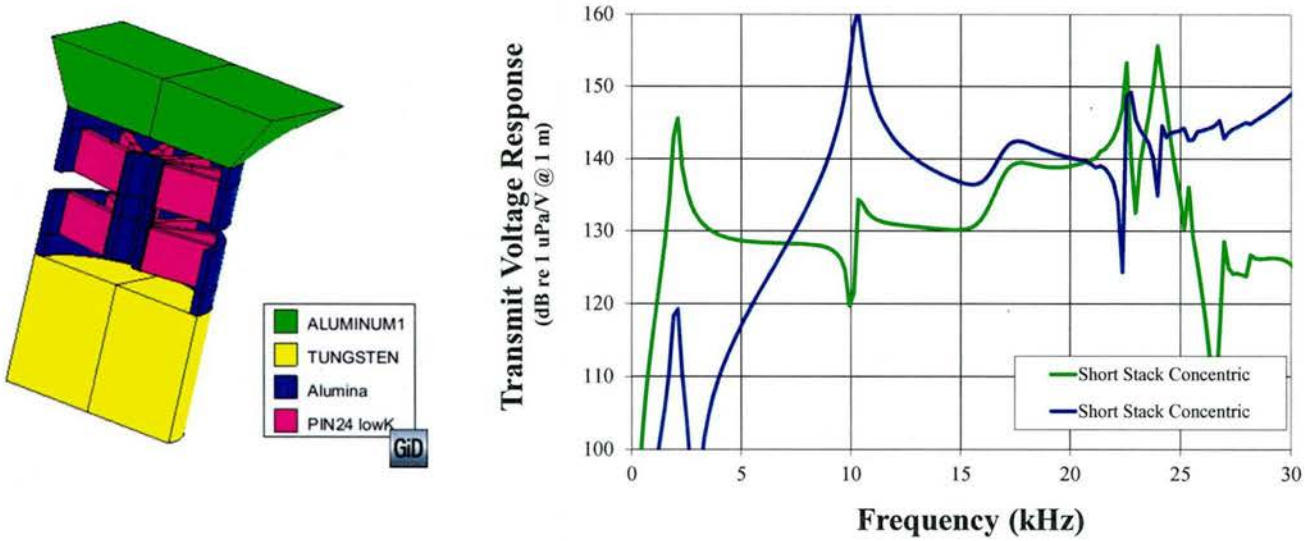

Figure 14 Two layer shear transducer with interior bridge/coupler mass (1/2 symmetry).

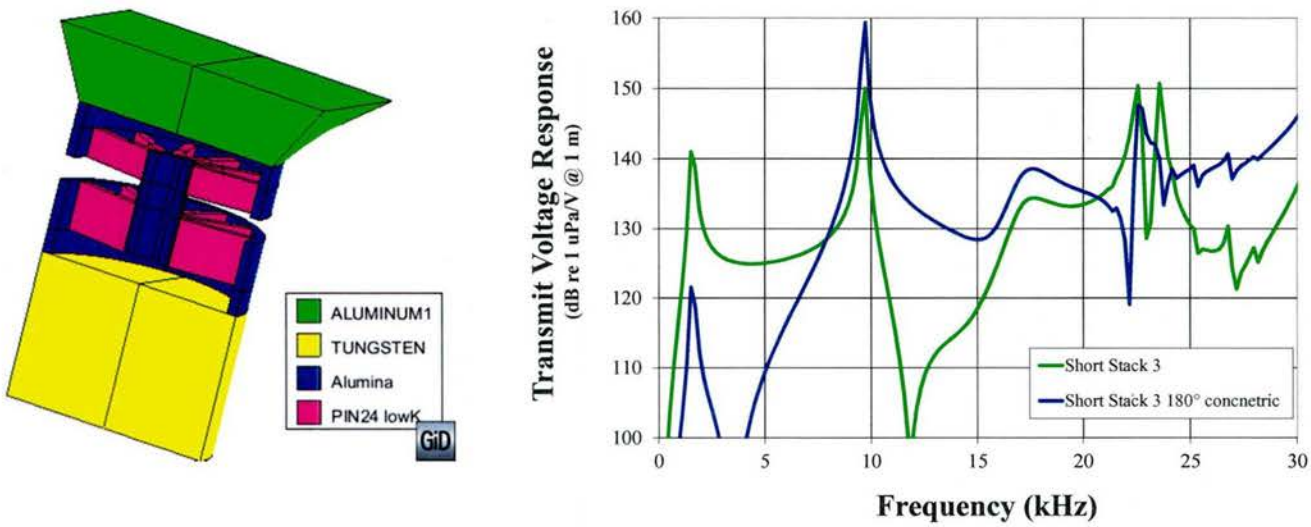

Figure 15 Interior coupled device with reduced width upper crystal layer (1/2 symmetry).

The options discussed above all utilize a series arrangement of the two crystal drivers. Figure 17and Figure 16 **Error! Reference source not found.** show parallel and series dual mode designs with small cross-sectional profile. These designs also demonstrate the frequency distribution achievable with varying polarity drive. These designs utilize a large volume of crystal, which provides high output power, but they are heavily mass loaded for low-frequency/high Qm peaks.

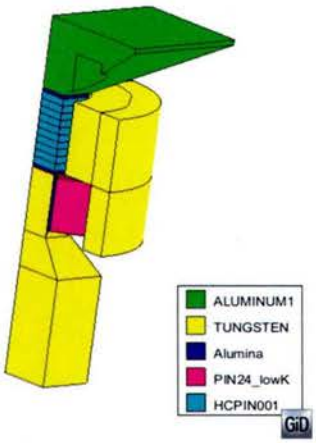

Type-B d33 above shear
Pseudo-Series with Rigid Coupler

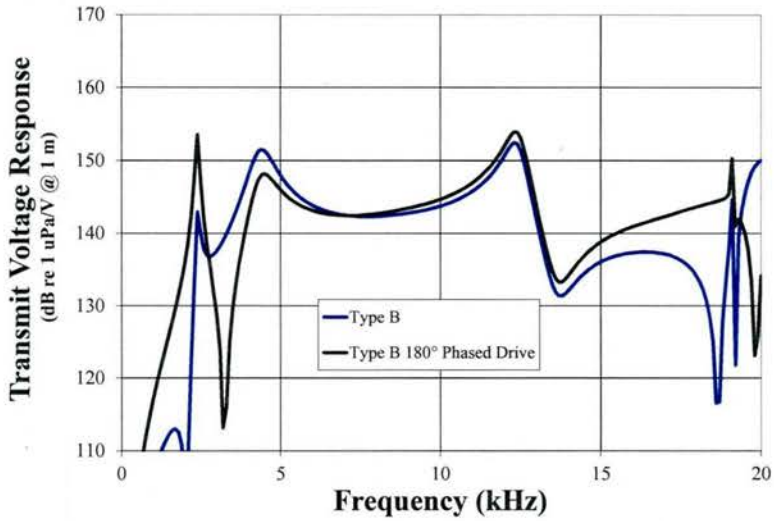

Figure 16 Series arrangement of d33 and d36 sections in small cross-section (1/4 symmetry).

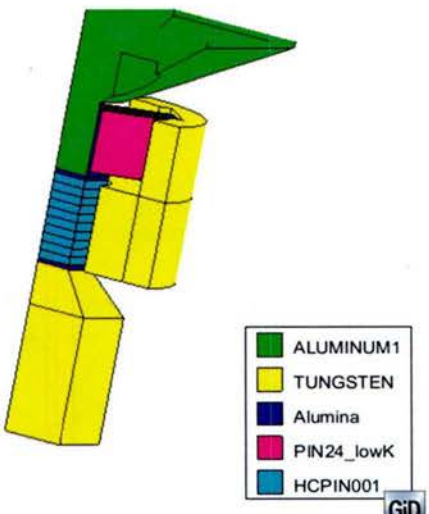

Type-A d33 below shear
True Parallel

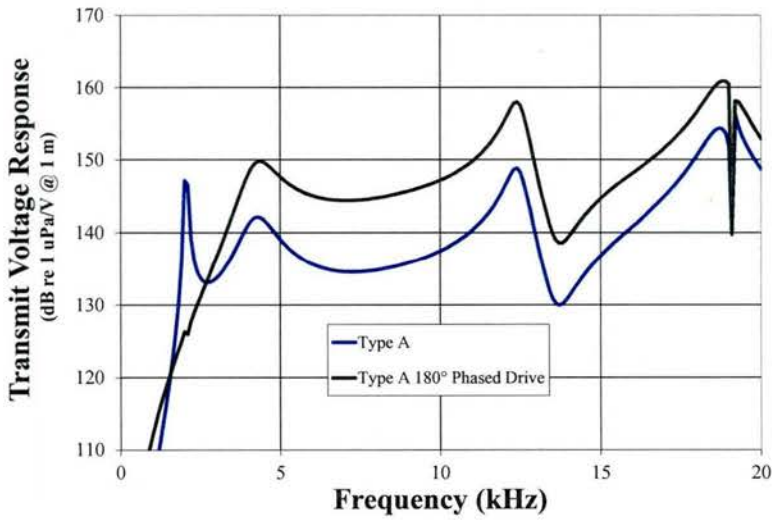

Figure 17 parallel arrangements of d33 and d36 sections in small cross-section (1/4 symmetry).

Another parallel arrangement is shown in Figure 18 with two independent tail masses each connected to two cantilevered crystals. To achieve the result shown, the upper tailmass is one-half the mass of the lower.

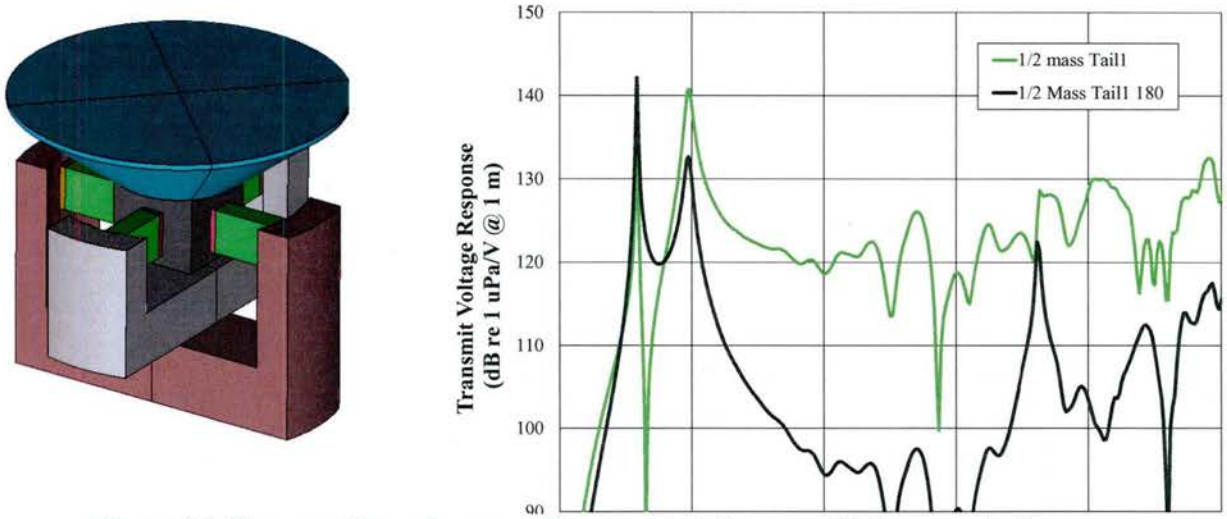

Figure 18 Two cantilever layers with separate tailmasses (full symmetry)

An alternative with wide, short profile can be made using two layers of cantilevered shear crystals nested in series radially, as shown in Figure 19. The combination of the crystals with the central mass makes one effective-length armature for extra low frequency. The second mode is a mechanical head flap. Therefore, in this case, 180° phasing gains nothing but actually disrupts the main mode. The third mode is actually the "coupler" mode. Adding more crystals increases the output power and the resonance frequency (Figure 20).

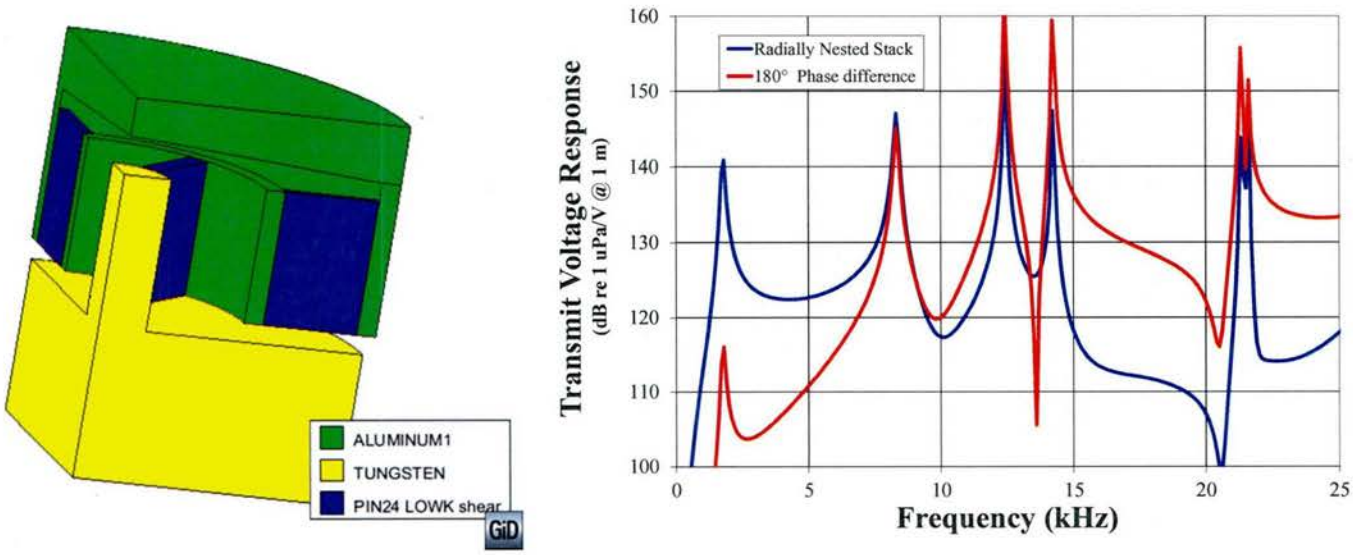

Figure 19 Radially nested shear layers (1/4 symmetry).

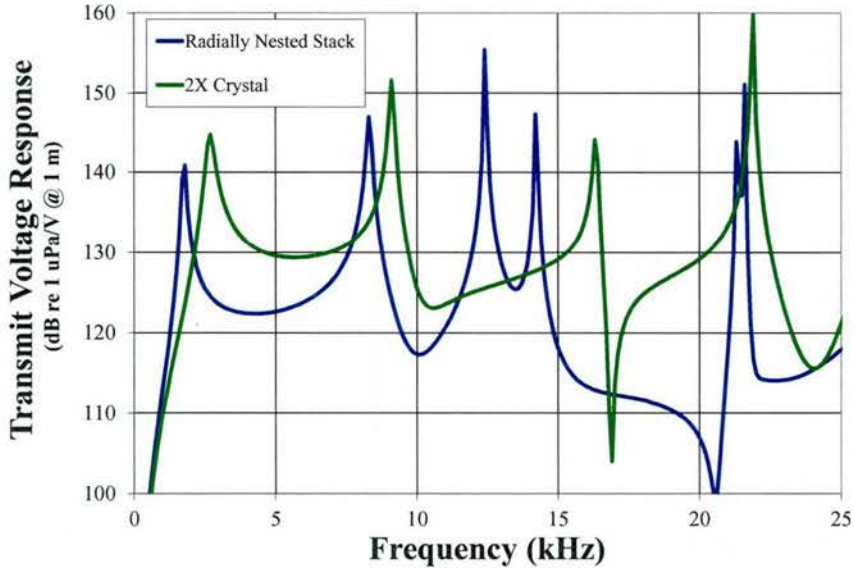

Figure 20 Radially nested shear layers with 2X crystal volume.

Figure 21 illustrates a possible configuration to use the cantilever motion of the crystals in a "scissoring" motion. The response is very broad band, but as the impedance and phase curves in Figure 22 illustrate, the effect is largely reactive, and results partly from mechanical modes of the headmass.

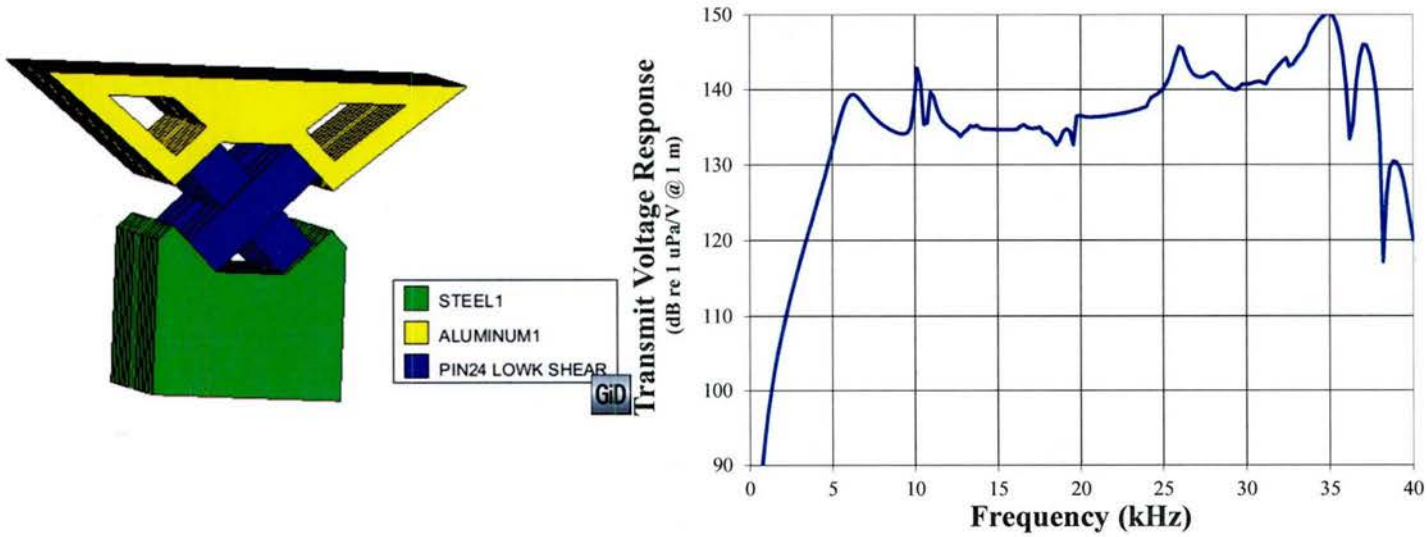

Figure 21 Scissor profile shear transducer (1/2 symmetry).

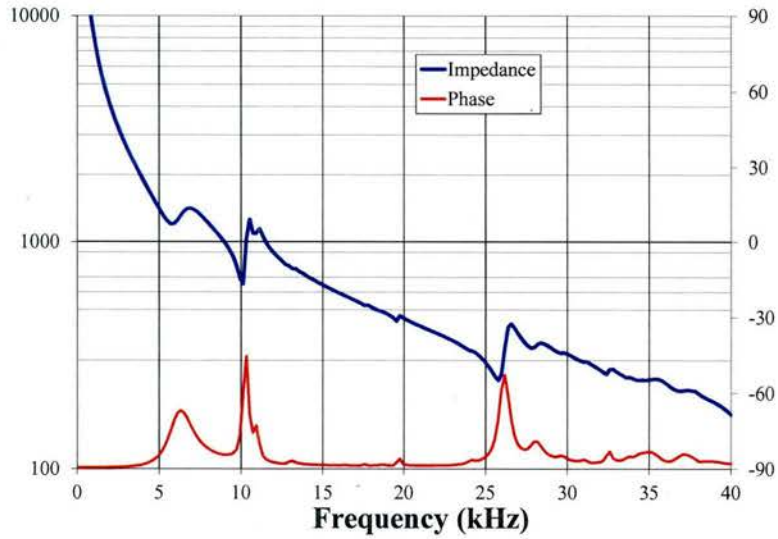

Figure 22 In-Water impedance and phase of the "Scissor" transducer.

In the course of these investigations, an alternative mechanism was uncovered for using the d_{36} motion to advantage. Figure 23 shows the loaded "Simple-Shear" motion of a cantilever configuration contrasted with the unconstrained "Free-Shear" motion that results from an unloaded state. In Figure 24 and Figure 25 the crystallographic orientation and resulting displacement motions are shown for what will be referred to as a Free-Shear design. In this orientation, the elongation motion direction $[0\bar{1}1]$ can be aligned with the desired device displacement direction, therefore, a stress bolt can be used in the device.

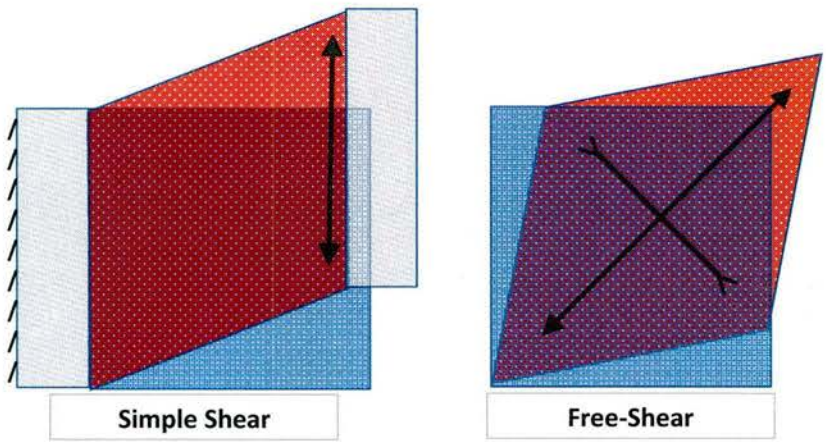

Figure 23 Simple-Shear and Free-Shear Displacements

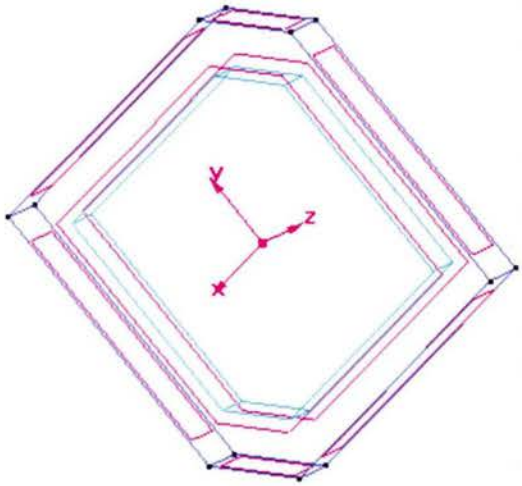

"Free-Shear" Polarization Orientation

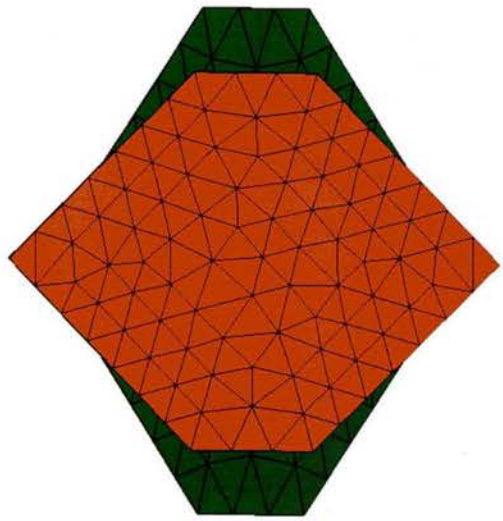

Free-Shear Displacement

Figure 24 "Free-Shear" crystallographic orientation and displacement model for d_{36} crystal.

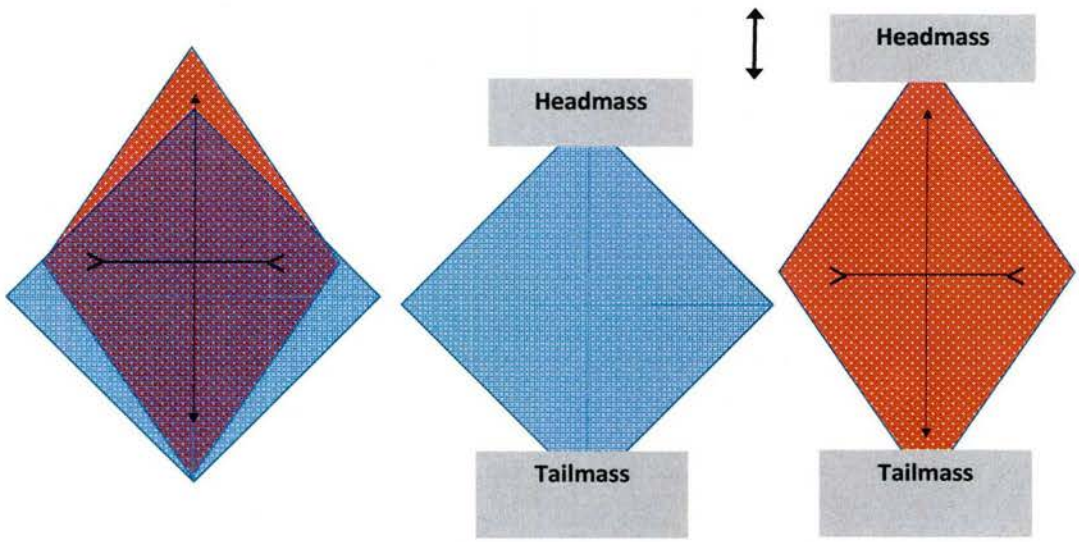

Figure 25 Free-Shear transducer concept.

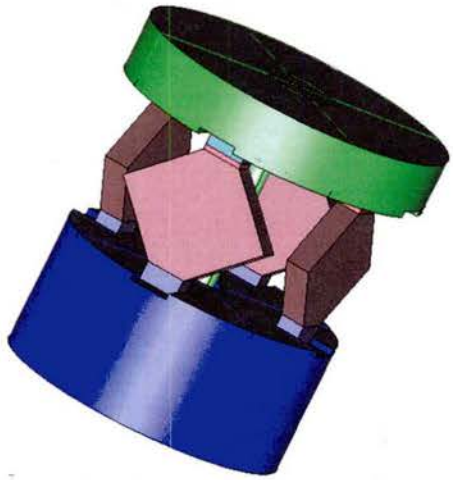

Figure 26 Four-crystal "Free-Shear" tonpilz model (full symmetry).

Figure 26 shows a model of a prototype "Tonpilz" type device using four Free-Shear crystals and a stress bolt.

Part drawings were produced and parts were procured. d_{36} crystals were obtained from HC Materials. Crystals were inspected, measured, and sorted for use in the transducer and evaluated for proper motion using a scanning laser vibrometer.

A photograph of the assembled prototype appears in Figure 27. The in-air impedance of the assembled device is shown in Figure 28. The modeled impedance is a very good match to the measured, but with a few high Qm spurious modes. The TVR of this "proof-of-concept" design is shown in Figure 29. The result is similar to the model, but contains some spurious modes, some of which were later attributed to modes in the single element housing that was used.

Figure 27 Photograph of Free-Shear prototype assembly.

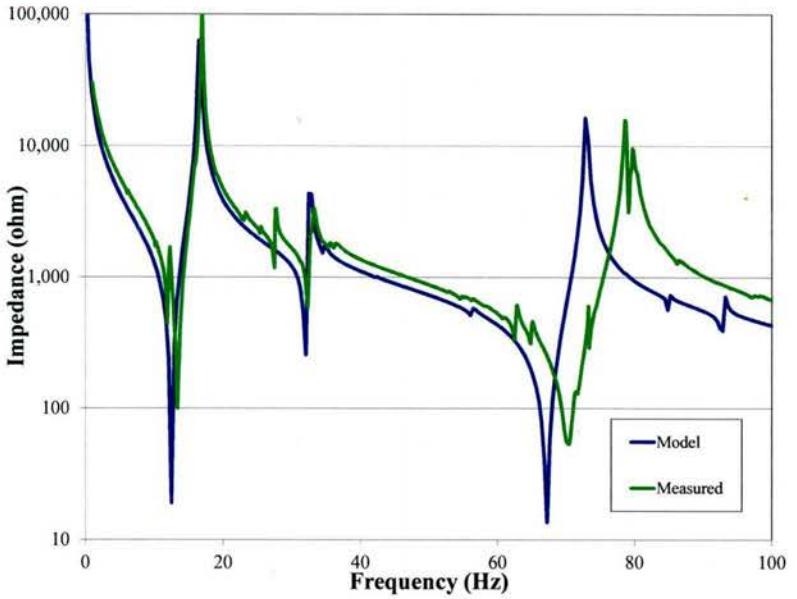

Figure 28 Measured and modeled in-air impedance of the Free-Shear tonpilz prototype.

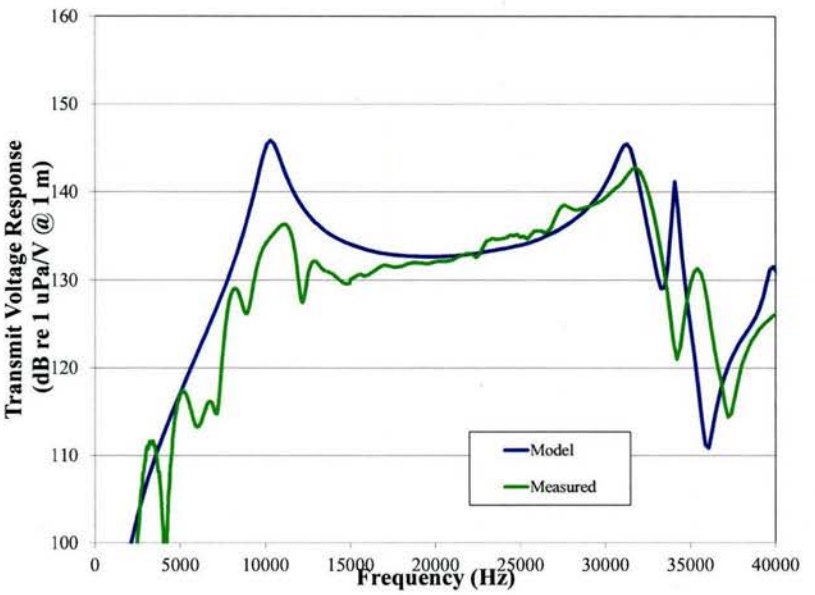

Figure 29 Measured and modeled transmit voltage response of the Free-Shear tonpilz prototype.

This configuration was then used to develop a multi-resonant prototype device, with two layers of Free-Shear crystals in series, as shown in Figure 30

Part drawings were produced and parts were procured. d_{36} crystals were obtained from HC Materials. Crystals were inspected, measured, and sorted for use in the transducer design and evaluated for proper motion using a scanning laser vibrometer.

The in-air impedance of the assembled device is shown in Figure 31. The modeled impedance is a very good match to the measured. The TVR of this "proof-of-concept" design is shown in Figure 32. The result is similar to the model.

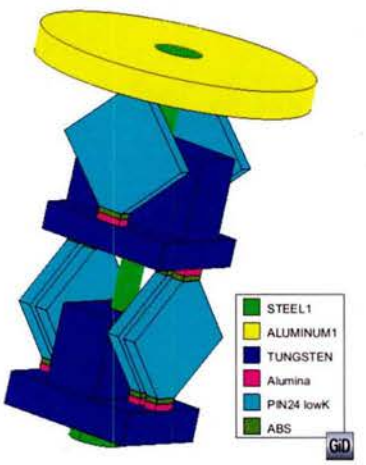

Figure 30 Photograph of the dual layer Free Shear tonpilz.

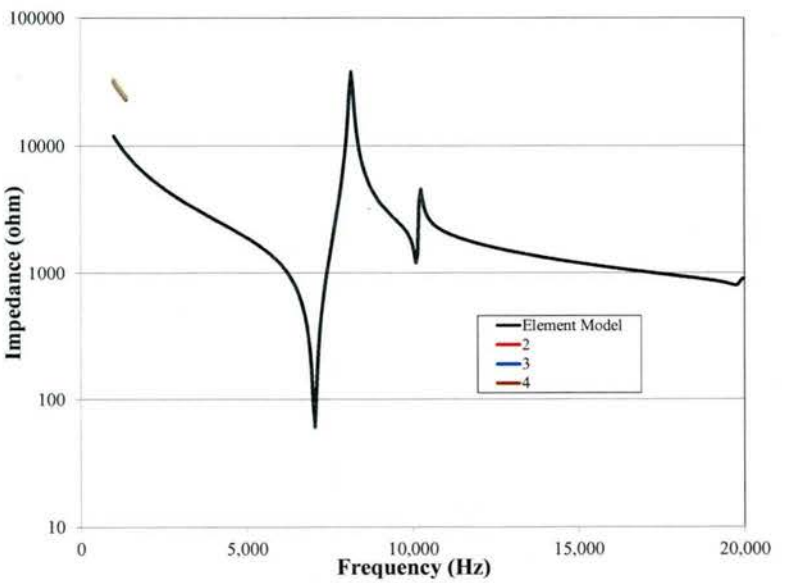

Figure 31 Modeled in-air impedance of the dual-layer Free-Shear tonpilz.

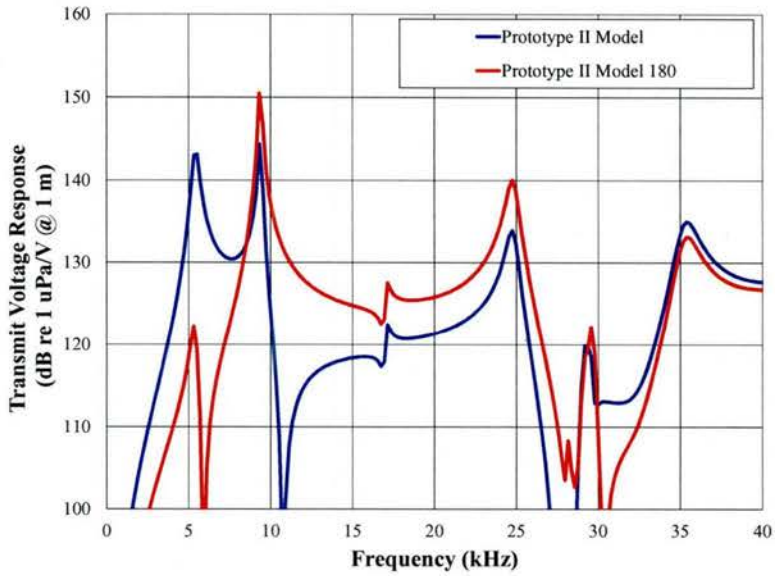

Figure 32 Measured and modeled transmit voltage response of the dual-layer Free-Shear tonpilz.

This orientation is sensitive to the alinement of the crystallographic directions with geometries. For example, for the crystal pieces used in the device above a modeling study shows the effects of misalignment of the crystallographic direction. Careful orientation and cutting by the vendor is required.

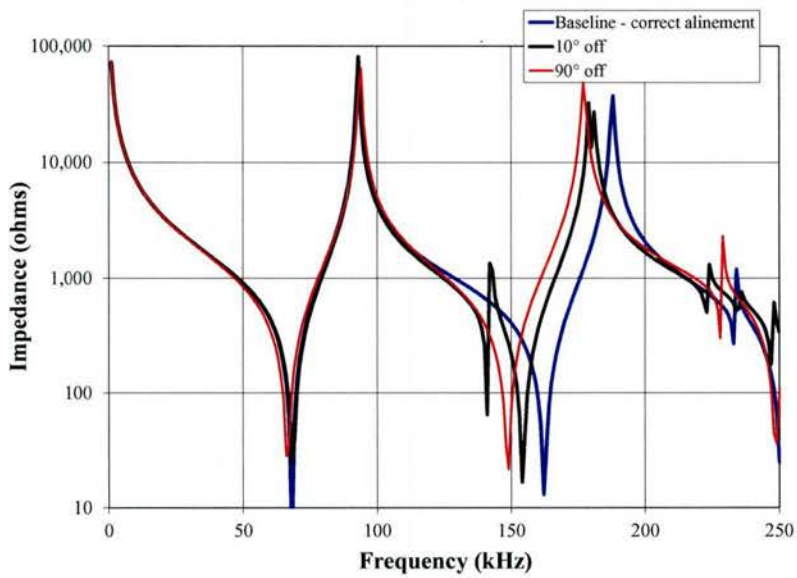

Variations of designs using the Free-Shear orientation have been explored in modeling studies, including scaling effects (Figure 33 and Figure 34) and multi-resonant designs (Figure 35 through Figure 37).

	Part1	Part2
Head Size	3" X 3"	1.3" X 1.3"
Crystal Size	.75" X .75"X.1"	.32" X .32"X.043"
Crystal count	14	14
Crystal Volume	.79 in3	0.06 in3

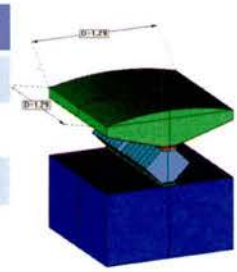

Figure 33 Scaling effects of another Free-Shear tonpilz design.

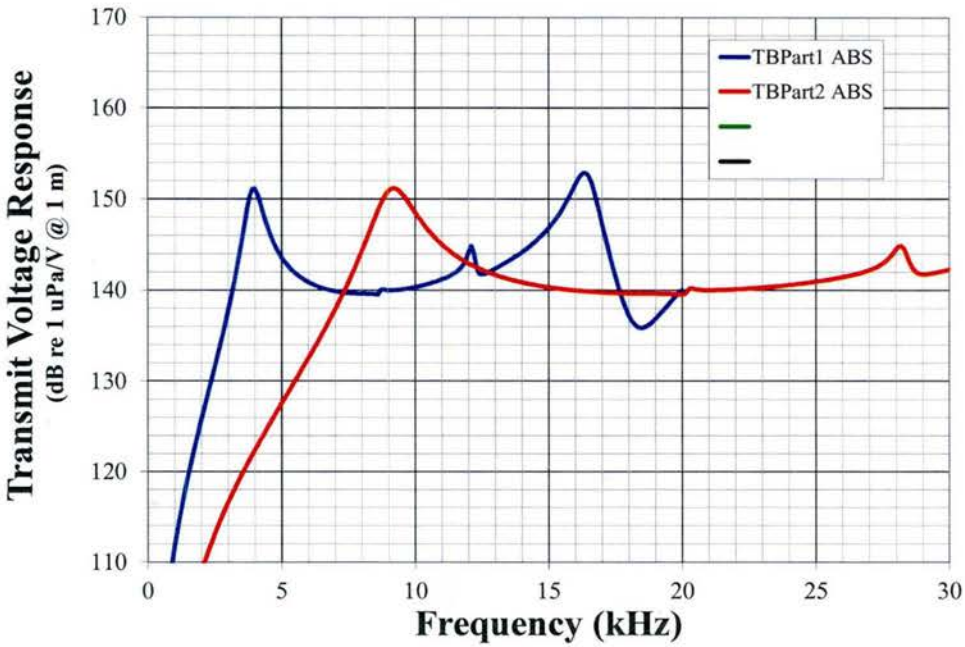

Figure 34 Transmit voltage response of the scaled Free-Shear tonpilz transducers.

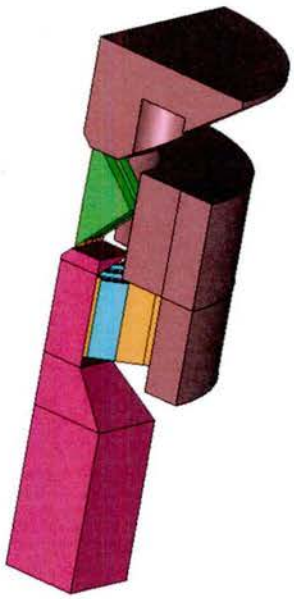

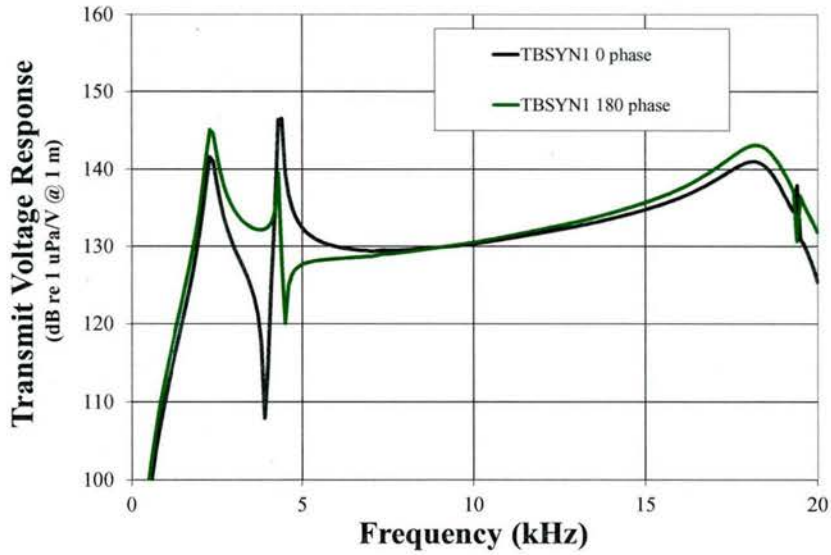

Figure 35 Modeled TVR of a series arrangement of Free-Shear and Simple-Shear section with small cross-section (1/4 symmetry).

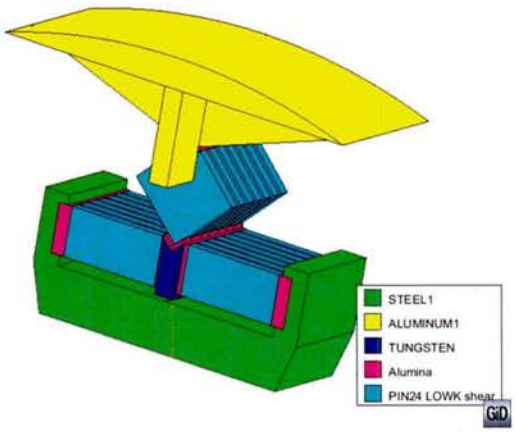

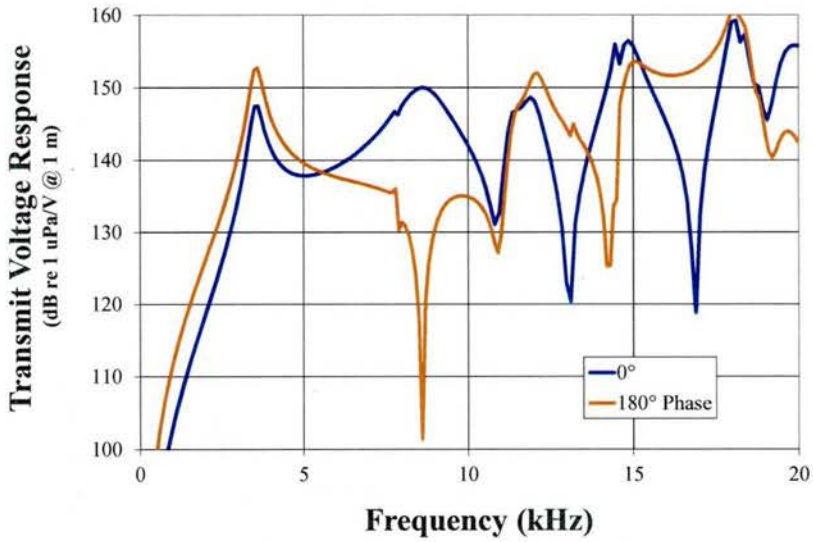

Figure 36 Free- and Simple-Shear components in a multi-resonant design (1/2 symmetry).

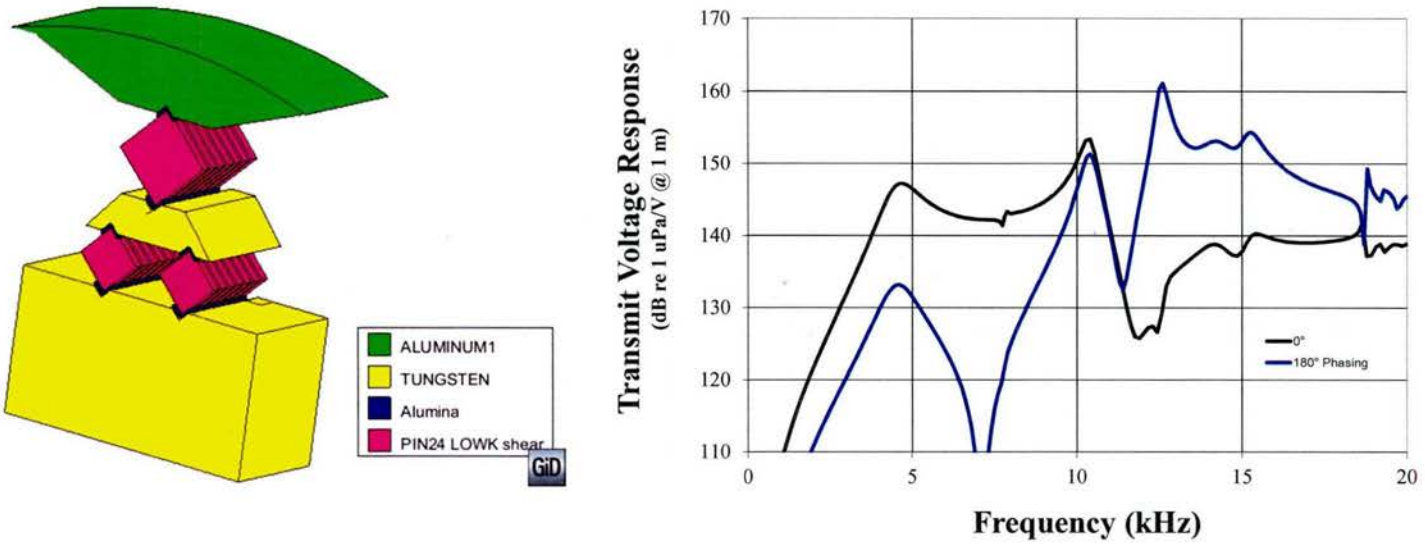

Figure 37 Multi-resonant stack of Free-Shear crystals (1/2 symmetry).

IMPACT/APPLICATIONS

Successful designs of very broad bandwidth transducers that are compact have many applications to Navy sonar.

SUMMARY

Multi-resonance shear designs have been explored using finite element modeling. The design space revealed several configurations of academic interest, including a new "free shear" configuration that has significant potential. Experimental prototyping of these designs confirm model predictions. Additional work is needed to fully vet the potential of these new designs.